Characterization of Oligomeric Intermediates in α-Synuclein Fibrillation: FRET Studies of Y125W/Y133F/Y136F α-Synuclein

ARTICLE *in* JOURNAL OF MOLECULAR BIOLOGY · NOVEMBER 2005

Impact Factor: 4.33 · DOI: 10.1016/j.jmb.2005.08.046 · Source: PubMed

6 AUTHORS, INCLUDING:

Joanna J. Kaylor
University of California, Los Angeles
12 PUBLICATIONS **498** CITATIONS
SEE PROFILE

Ghiam Yamin
University of California, San Diego
22 PUBLICATIONS **1,248** CITATIONS
SEE PROFILE

Dong-Pyo Hong
University of South Florida
24 PUBLICATIONS **1,043** CITATIONS
SEE PROFILE

doi:10.1016/j.jmb.2005.08.046 J. Mol. Biol. (2005) 353, 357–372

JMB

Available online at www.sciencedirect.com

SCIENCE DIRECT®

ELSEVIER

Characterization of Oligomeric Intermediates in α-Synuclein Fibrillation: FRET Studies of Y125W/Y133F/Y136F α-Synuclein

Joanna Kaylor, Nika Bodner, Shauna Edridge, Ghiam Yamin Dong-Pyo Hong and Anthony L. Fink*

Department of Chemistry and Biochemistry, University of California, Santa Cruz, CA 95064, USA

*Corresponding author

The aggregation of α-synuclein is believed to be a critical step in the etiology of Parkinson's disease. A variety of biophysical techniques were used to investigate the aggregation and fibrillation of α-synuclein in which one of the four intrinsic Tyr residues was replaced by Trp, and two others by Phe, in order to permit fluorescence resonance energy transfer (FRET) between residues 39 (Tyr) and 125 (Trp). The mutant Y125W/Y133F/Y136F α-synuclein (one Tyr, one Trp) showed fibrillation kinetics similar to that of the wild-type, as did the Y125F/Y133F/Y136F (one Tyr, no Trp) and Y39F/Y125W/Y133F/Y136F (no Tyr, one Trp) mutants. Time-dependent changes in FRET, Fourier transform infrared, Trp fluorescence, dynamic light-scattering and other probes, indicate the existence of a transient oligomer, whose population reaches a maximum at the end of the lag time. This oligomer, in which the α-synuclein is in a partially folded conformation, is subsequently converted into fibrils, and has physical properties that are distinct from those of the monomer and fibrils. In addition, another population of soluble oligomers was observed to coexist with fibrils at completion of the reaction. The average distance between Tyr39 and Trp125 decreases from 24.9 Å in the monomer to 21.9 Å in the early oligomer and 18.8 Å in the late oligomer. Trp125 remains solvent-exposed in both the oligomers and fibrils, indicating that the C-terminal domain is not part of the fibril core. No FRET was observed in the fibrils, due to quenching of Tyr39 fluorescence in the fibril core. Thus, aggregation of α-synuclein involves multiple oligomeric intermediates and competing pathways.

Keywords: Parkinson's disease; protein aggregation; amyloid; fluorescence; protofibrils

Introduction

Parkinson's disease (PD) is the second most common neurodegenerative disease: the pathological hallmark of PD is the presence of filamentous inclusions, Lewy bodies, which are present in the substantia nigra and other regions of the brain.[1] Parkinson's disease is believed to have a multifactorial etiology, including genetic and environmental factors,[2–5] in which the aggregation of α-synuclein plays a critical role.[2,3,6–9] The 140 amino acid residue protein is natively unfolded and has two chemically distinct regions in its sequence: the N-terminal region includes the first 93 residues and is characterized by seven imperfect repeats of 11 residues, predicted to form amphiphilic helices, and corresponding to an apolipoprotein binding motif. The C-terminal region is highly acidic and predicted to lack ordered secondary structure.[10,11]

The sigmoidal kinetics of fibrillation suggest a nucleation-dependent polymerization mechanism. The existence of a critical amyloidogenic partially folded intermediate has been demonstrated.[12] It has

Abbreviations used: ANS, 1-anilinonaphthalene-8-sulfonic acid; ATR-FTIR, attenuated total reflectance Fourier transform infrared; EM, electron microscopy; FRET, fluorescence resonance energy transfer; FSD, Fourier self-deconvolution; PD, Parkinson's disease; ThT, thioflavin.

E-mail address of the corresponding author: enzyme@cats.ucsc.edu

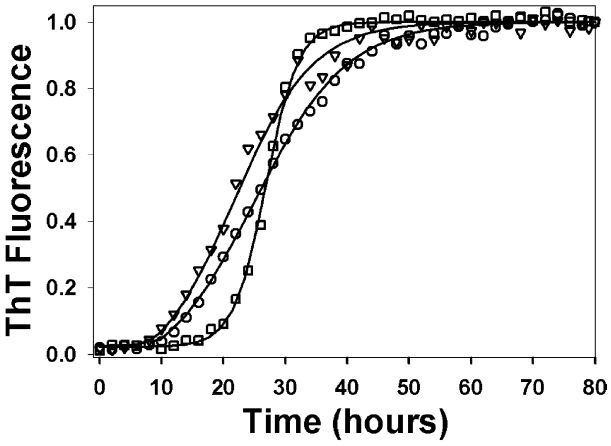

Figure 1. Comparison of the kinetics of fibrillation of wild-type (squares), Y125W/Y133F/Y136F (inverted triangles), and Y39F/Y125W/Y133F/Y136F (circles) α-synuclein by thioflavin T fluorescence. Measurements were performed at 37 °C in 20 mM buffer (PBS, pH 7.5), 100 mM NaCl, and 1 mg/ml of protein on a fluorescence plate reader (600 rpm shaking with a diameter of 2 mm).

been suggested that oligomeric precursors of fibrils may be more responsible for Parkinson's disease than the fibrils themselves.[13,14]

An essential question is how a natively disordered protein transforms into the highly organized β-strand conformation of a fibril? Internal probes of α-synuclein aggregation could provide valuable insight into its fibrillation. Since α-synuclein lacks Trp residues, one such probe would be the naturally fluorescent Trp residue. The four tyrosine residues in wild-type α-synuclein provide optimal sites for the introduction of tryptophan and phenylalanine, which have physical properties similar to those of tyrosine. The four tyrosine residues in wild-type human α-synuclein are at positions 39, 125, 133, and 136, spanning both of the structurally distinct regions of the protein.

Here, we report the structural and fibrillation properties of the α-synuclein mutant Y125W/Y133F/Y136F. This mutant has physical properties very similar to those of wild-type α-synuclein, including the ability to form fibrils with similar kinetics and morphology. This mutant contains a new environmental probe at position 125, and replaces the remaining wild-type tyrosine residues with phenylalanine, except for the tyrosine residue at position 39. Thus, the mutant permits the use of fluorescence resonance energy transfer (FRET) to measure the distance between Tyr39 and Trp125. The efficiency of energy transfer is found by comparing the mutant Y125W/Y133F/Y136F to the mutant Y39F/Y125W/Y133F/Y136F, which has no energy transfer possible, since it lacks tyrosine.

FRET is a well-established technique used to measure intra- and intermolecular distances in proteins. There are multiple reasons why introducing tyrosine and tryptophan as a FRET pair to α-synuclein is desirable. First, these naturally occurring amino acid side-chains are expected to have only minor influence on the structure and fibrillation of the protein. Second, the fibrillation process occurs over many hours, facilitating spectroscopic monitoring. Third, energy transfer is expected, since unfolded α-synuclein at pH 7.5 and 100 mM NaCl has a Stokes radius of 31.8(±0.4) Å and a radius of gyration of 41(±1) Å.[15] These are within the Förster defined distances at which energy transfer can occur and is measurable. Energy transfer between Tyr39 and Trp125 allows distance calculations between the two distinct regions of α-synuclein (the potential helical repeat region and the C-terminal unfolded tail). The biophysical studies reported here for Y125W/Y133F/Y136F reveal the existence of a transient oligomer, whose population reaches a maximum at the end of the lag time, and whose properties are distinct from those of the monomer and fibrils. W125 remains solvent-exposed in this oligomeric intermediate, as well as in the fibrils, indicating that the C-terminal domain is not part of the fibril core.

Results

Comparison of fibrillation of wild-type α-synuclein to the mutants

The kinetics of fibril formation and fibril morphology for Y125W/Y133F/Y136F (one Tyr, one Trp) α-synuclein were compared to wild-type (four Tyr) and the tyrosine-free homolog Y39F/Y125W/Y133F/Y136F (no Tyr, one Trp) α-synuclein. Figure 1 shows the time-dependent changes in the thioflavin (ThT) fluorescence during the process of fibril formation for wild-type *versus* the different mutants under the same experimental conditions at 37 °C and pH 7.5, using the plate-reader. The fibrillation

Table 1. Comparison of the fibrillation kinetics of wild-type and mutant α-synucleins at pH 7.5, 100 mM NaCl, 37 °C

	Mass		Kinetics		
Protein	Expected	Observed	$t_{½}$ (h)	Lag time (h)	Elongation rate (h^{-1})
Wild-type	14,460	14,462±2	26.9±0.1	21.6±0.1	0.38±0.04
Y125W/Y133F/Y136F	14,451	14,450±2	21.7±0.3	9.1±0.2	0.16±0.19
Y39F/Y125W/Y133F/Y136F	14,435	14,434±2	25.0±0.2	10.1±0.2	0.13±0.16

kinetics for all three proteins exhibit characteristic sigmoidal curves, which have an initial lag phase, a subsequent growth phase, and a final equilibrium phase. Such curves are consistent with the nucleation-dependent polymerization model, in which the lag corresponds to the nucleation phase and the exponential part corresponds to fibril growth.[12] The fibrillation kinetics of the mutants were similar to those of the wild-type, except that the lag times and elongation rates for the mutants were approximately twofold less than those of the wild-type. Table 1 shows the calculated kinetic parameters for each protein based on the ThT fluorescence assays. The faster nucleation and slower fibril elongation of the mutants is attributed to the changed hydrophobicity of the mutants compared to that of the wild-type. For the subsequent experiments, where supernatant and pellet were separated, incubation was done in vials, with a stirring bar. This led to less agitation, which was manifested by slower kinetics of fibrillation (the lag for the FRET mutant is ∼44 h, see Figure 4): it is well known that the kinetics of protein aggregation are very dependent on agitation.

To further compare the mutants to wild-type α-synuclein, negatively stained transmission electron microscopy (EM) images were made to compare the fibril morphology (Figure 2). EM images show that the fibrils produced by the mutants are similar to those of wild-type, indicating the morphology of the fibrils was not significantly affected by the amino acid substitutions. All mutant fibrils analyzed have the characteristic rod-like shape and were approximately 10(±3) nm wide and 0.2–2 μm long, analogous to wild-type α-synuclein fibrils.

Attenuated total reflectance Fourier transform infrared spectroscopy (ATR-FTIR) analysis of Y125W/Y133F/Y136F fibrillation

ATR-FTIR analysis was used to investigate the secondary structure of Y125W/Y133F/Y136F during fibrillation. By using ATR-FTIR, very small samples with low concentrations of protein can be used. Spectra of the amide I region (1700–1600 cm^{-1}), which is especially sensitive to β-structure, were collected. Samples were taken at selected times during the incubation of Y125W/Y133F/Y136F at 37 °C and pH 7.5, and separated into pellet and supernatant fractions by centrifugation. Figure 3(a) shows the amide I region spectra at different time intervals for the supernatant: the spectra are typical of a substantially unfolded protein. The major structural changes observed with increasing time of incubation occur around 1630 cm^{-1}, reflecting changes in β-structure. The amount of β-structure increases initially and then decreases, suggesting build-up and decay of a transient intermediate. We term this the early oligomeric intermediate (the oligomeric association state was confirmed by dynamic light-scattering, see Figure 6). The differences in the area-normalized amide I spectra

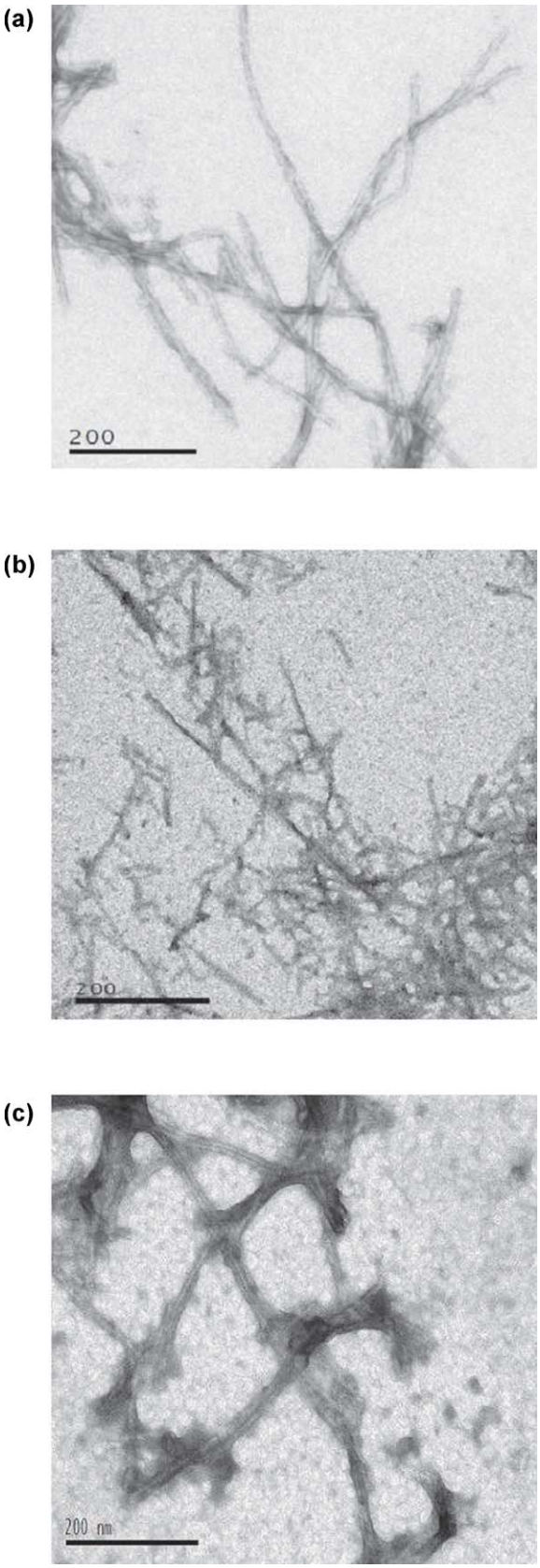

Figure 2. Negatively stained electron microscope images of fibrils formed by (a) wild-type, (b) Y125W/Y133F/Y136F, and (c) Y39F/Y125W/Y133F/Y136F α-synuclein. The scale bar for (a)–(c) represents 200 nm. Fibrils were prepared with the same conditions as in Figure 1.

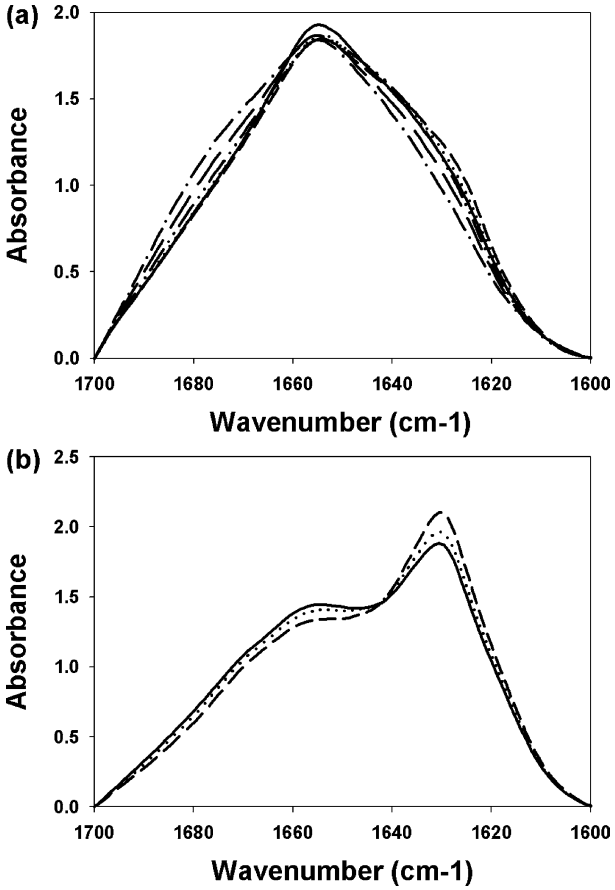

Figure 3. ATR-FTIR spectra of the amide I region as a function of time during the incubation/fibrillation of Y125W/Y133F/Y136F α-synuclein showing changes in the secondary structure: (a) supernatant; (b) pellet samples. The protein was incubated at 37 °C in 20 mM sodium phosphate (pH 7.5), 100 mM NaCl, and 2 mg/ml of protein with stirring. Samples were prepared by removing aliquots from the incubation mixture centrifuged to separate the pellet and the supernatant. Spectra are normalized for area. Line codes: (a) time zero (continuous), 8 h (broken, long dashes), 16 h (broken, medium dashes), 48 h (broken, short dashes), 72 h (dotted), and 125 h (dot-dash); (b) 56 h (continuous), 76 h (dotted), and 125 h (broken).

with time, seen in Figure 3(a), suggest heterogeneity in the structure of these transient intermediates, with less, or different, β-structure in the later species.

The pellet samples show small changes in secondary structure in the amide I region with increasing time of incubation (Figure 3(b)). Changes occur in the absorbance around 1630 cm^{-1} (increase) and 1655 cm^{-1} (decrease). The distinctive peak around 1630 cm^{-1} corresponds to an increase in β-sheet structure as the fibrils form and elongate. The decrease in the band around 1655 cm^{-1} represents a decrease in the disordered structure, and occurs concurrently with the rise of the signal around 1636 cm^{-1}.

The changes in the β-structure of the protein species present in the supernatant and pellet samples are particularly revealing when plots are made of the absorbance of the sample at 1630 cm^{-1} as a function of time. Figure 4 shows these plots superimposed with the ThT fluorescence curve, to permit comparison of the overall fibrillation process to the changes occurring in secondary structure. Figure 4(a) shows the structural changes in the supernatant: before the fibril elongation phase is reached, there is a build up of β-structure in the supernatant population. The increase and then decrease in the 1630 cm^{-1} absorbance is consistent with the formation of an intermediate during the lag time with increased β-structure, which subsequently decays as fibrils are formed. The maximum amount of the intermediate is reached toward the end of the lag time. Figure 4(b) shows for the pellet samples an increase in the amount of β-structure parallel with the increase in ThT fluorescence, reflecting the formation of the fibrils.

The amide I region infrared spectra can be used to analyze the amount of secondary structure by

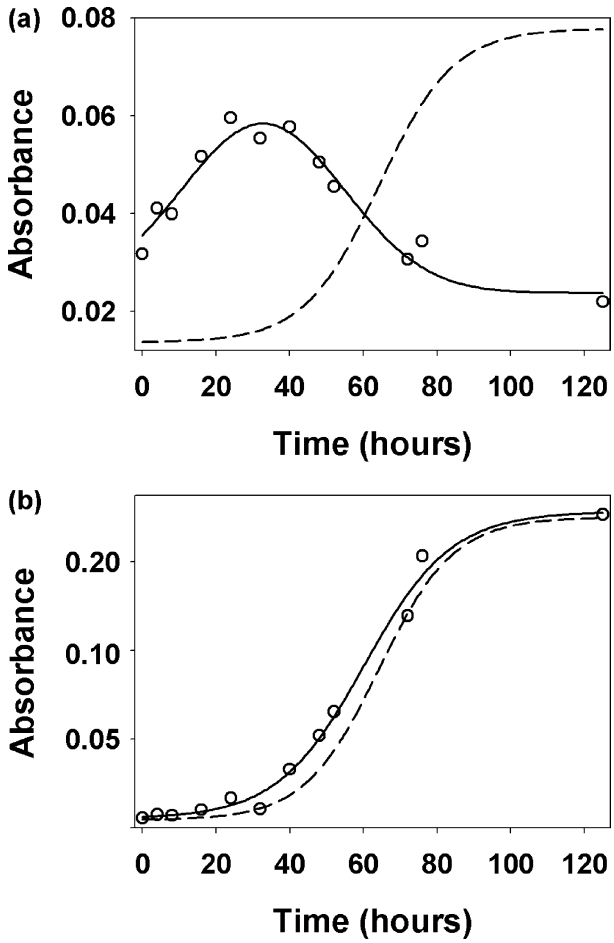

Figure 4. Changes in the β-structure during the aggregation of Y125W/Y133F/Y136F α-synuclein. Plots of absorbance at 1630 cm^{-1} (open circles) against time for (a) supernatant and (b) pellet samples. The ThT fluorescence trace (broken line) is shown for comparison. Samples were prepared as described for Figure 3.

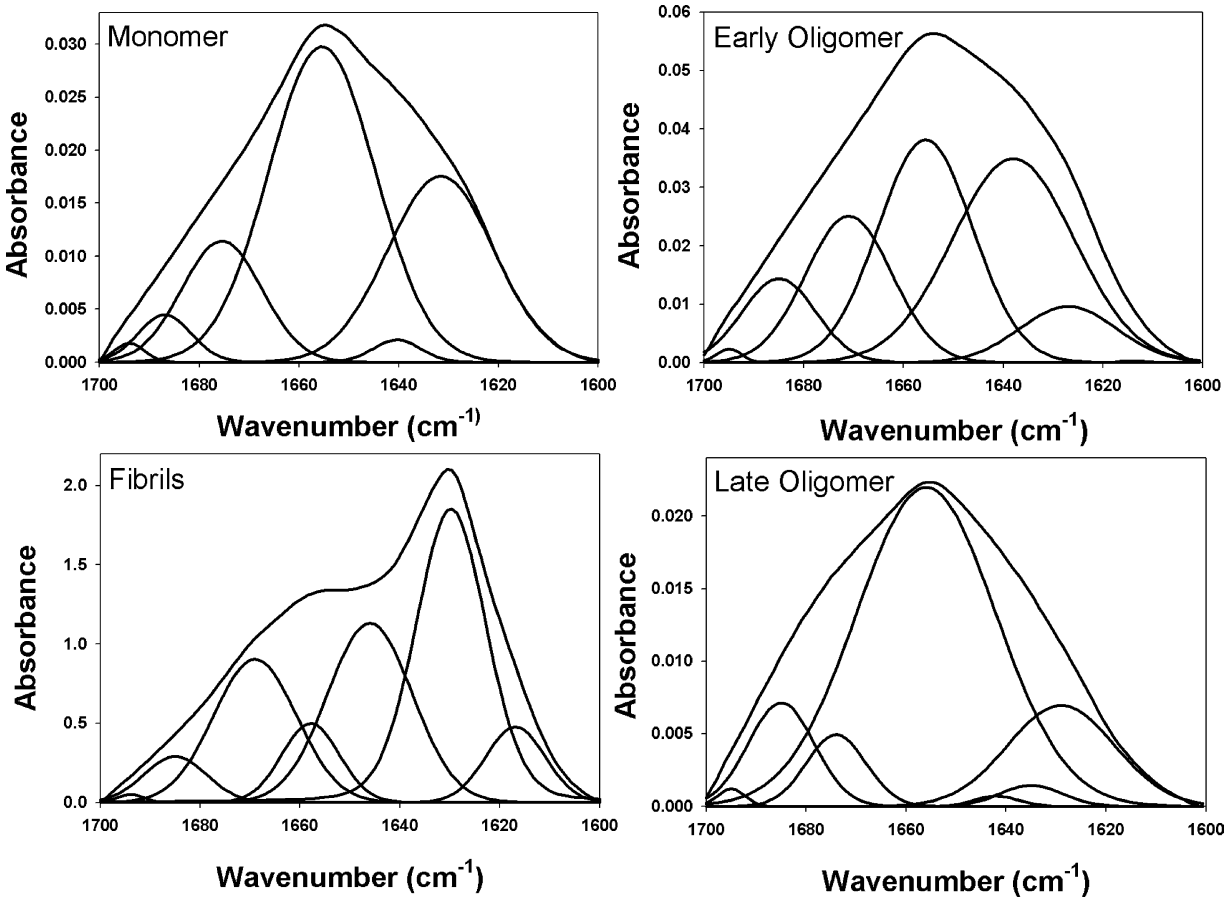

Figure 5. ATR-FTIR secondary structure analysis of key species in the fibrillation of Y125W/Y133F/Y136F α-synuclein. Samples for the monomer were taken at time zero, for the early oligomeric species at 32 h, for the fibrils at 125 h, and for the late oligomeric species at 76 h. Spectra were deconvoluted and curve-fit to ascertain the secondary structure composition (Table 2). Peaks in the region 1610–1640 cm^{-1} are mostly from β-structure, those around 1655 cm^{-1} from disordered structure, and from 1665 cm^{-1} to 1700 cm^{-1} mostly from loops and turns.

deconvolution and curve-fitting.[16,17] Briefly, individual secondary structure components can be obtained from amide I spectra using a combination of deconvolution and curve-fitting procedures (see Materials and Methods for details). In essence, the position and number of components is determined using both second derivatives and Fourier self-deconvolution (FSD). If both techniques are in agreement for the position of a particular component, then this information is used in the curve-fitting routine. Once the component band positions are identified, they can be assigned to particular secondary structure, using an empirically based data set. Deconvolution was applied to spectra during key points of the fibrillation process for Y125W/Y133F/Y136F: the initial monomeric species, the early oligomers, the fibrils, and the non-fibrillating late oligomers (see below). Figure 5 shows the deconvolution and curve-fit of these spectra for key populations, and the resulting secondary structure analysis is summarized in Table 2. Compared to monomeric wild-type α-synuclein,[15] the FRET mutant appears to already have an appreciable amount of β-structure present, as is indicted by a small shoulder at 1630 cm^{-1} and less absorbance at 1655 cm^{-1}. This suggests that the

Table 2. Secondary structure comparison of key populations during the fibrillation of Y125W/Y133F/Y136F α-synuclein in 100 mM NaCl at pH 7.5, 37 °C

	% β-Structure	% Disordered	% Turn	Sample time (h)
Monomers	27	56	17	0
Early oligomers	43	30	27	32
Fibrils	43	32	25	125
Late oligomers	18	65	17	76

Deconvolution error ±5–6% for areas.

presence of the Trp and/or the loss of the two Tyr residues, leads to a small decrease in disordered structure in the mutant compared to the wild-type. The early oligomeric intermediate contains significant amounts of β-structure. Comparison of the secondary structure of these early oligomers to the fibrils shows the β-structure contribution in both to be very similar (43(±5)%) with only the percentage disordered and turns changing slightly. However, the nature of the β-structure is quite different, as can be seen from Figure 5. The increased peak height around 1630 cm^{-1} due to the extended β-structure is present only in the fibrils. The non-fibrillar soluble late oligomer population shows the least amount of β-structure overall, with only 35(±5)% being attributed to ordered secondary structure.

Dynamic light-scattering shows α-synuclein forms a transient intermediate

We used dynamic light-scattering in order to confirm that the early changes in the FTIR spectra did indeed correspond to formation of a transient oligomeric intermediate. The data reveal several interesting features (Figure 6). For example, the concentration of the early intermediate reaches a peak at the end of the lag phase, with a concentration of ~20% of the total soluble protein. The concentration of this oligomeric intermediate becomes significant by 10 h, and disappears rapidly during the fibril elongation phase. A different, smaller, oligomer is present during the later stages of the fibril growth and remains after completion of the fibrillation process. We call this the late oligomer.

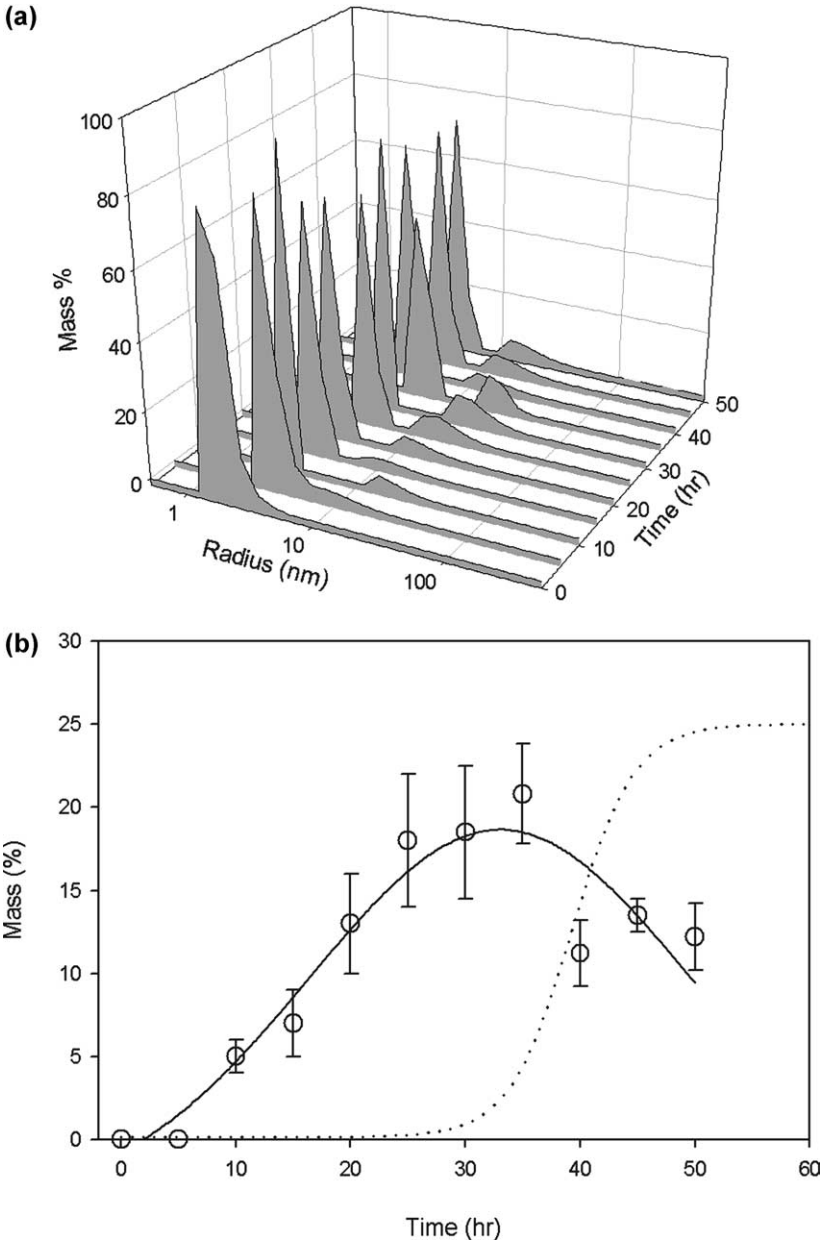

Figure 6. Build-up of oligomers during the incubation of Y125W/Y133F/Y136F α-synuclein. Changes in dynamic light-scattering as a function of time during the incubation of wild-type α-synuclein. (a) The time-dependent scattering profiles as mass percentage against Stokes radius. (b) A comparison of the amount of oligomer as a function of incubation time, against the formation of fibrils as measured by ThT signal (dotted line). The monomer has R_s = 2.6 nm, the early oligomer has R_s ~10 nm.

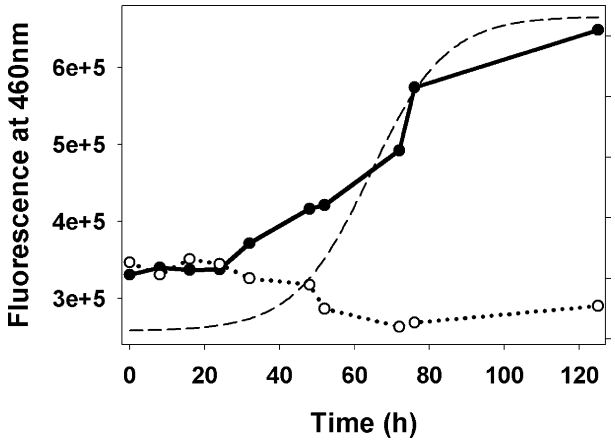

Figure 7. Changes in ANS binding as a function of time during the fibrillation of Y125W/Y133F/Y136F α-synuclein. Data for the supernatant (dotted line, open circles) and pellet (continuous line, filled circles) are shown, along with the ThT fluorescence (broken line) for comparison. ANS excitation was at 350 nm and the emission was measured at 460 nm.

Structural characterization of Y125W/Y133F/Y136F by ANS binding

The fluorescent dye 1-anilinonaphthalene-8-sulfonic acid (ANS) can be used to detect the presence of partially folded globular proteins.[18] ANS binds to solvent-exposed hydrophobic clusters, resulting in an increase in ANS fluorescence intensity. Aliquots of the incubation mixture of Y125W/Y133F/Y136F were diluted in ANS buffer solution. These were then excited at 350 nm and the emission was measured at 460 nm (Figure 7). In the pellet samples, the ANS fluorescence increases constantly as the fibrillation progresses, reflecting an increase of solvent-exposed hydrophobic clusters. The supernatant fractions show slightly increased ANS fluorescence at early times in the fibrillation but the fluorescence intensity begins to decrease as fibril elongation starts to take place. The changes in ANS fluorescence of the supernatant parallel the changes in β-structure observed by FTIR, and are attributed to the buildup and decrease in population of the early oligomeric intermediate. The soluble oligomers present at the end of the incubation have negligible ANS binding, consistent with their mostly disordered structure from FTIR.

Intrinsic tryptophan fluorescence of Y125W/Y133F/Y136F

The mutant Y125W/Y133F/Y136F α-synuclein has a single tryptophan residue at position 125 in the C-terminal region of the protein. Tryptophan is the most fluorescent amino acid and fluoresces readily when excited at 290 nm to give an emission maximum between 310 nm and 360 nm, depending on its environment. Tryptophan emission is typically around 355 nm for unfolded proteins, due to solvent exposure, and can be blue shifted as much as 30 nm or more if buried deeply. Thus, the wavelength maximum for tryptophan emission can be used to monitor the solvent exposure of Trp125 during fibrillation. Samples were taken approximately every 4 h during incubation for 125 h. Pellet and supernatant were separated, samples were excited at 290 nm and the fluorescence emission was observed from 300–440 nm. Since there is negligible excitation of Tyr at this wavelength, there will be no contributions from energy transfer. As fibrillation progressed, the intensity of the intrinsic tryptophan emission spectra of the pellet increased in parallel with the increase in ThT fluorescence. However, the wavelength of the emission maxima did not change, and remained at 352 nm for the entire fibrillation. This indicates a solvent-exposed environment for Trp125 in the fibrils.

The intensity of the tryptophan emission decreased as the incubation time progressed, reflecting the decrease in protein in the supernatant fractions, and there was a small blue shift from 356 nm to 352 nm in λ_{max} at the later stages of the reaction. The blue shift indicates a slightly less solvent-exposed tryptophan residue in the late oligomeric intermediate found in the supernatant at long incubation times.

Energy transfer in Y125W/Y133F/Y136F

Y125W/Y133F/Y136F α-synuclein has a single tyrosine donor at position 39 and a single tryptophan acceptor at position 125. Tryptophan, when present, usually dominates the fluorescence spectra of a protein, since it quenches tyrosine emission by fluorescence resonance energy transfer,[19] due to tyrosine emission overlapping with tryptophan absorption. The amount of energy transferred is dependent on the distance and orientation between tyrosine and tryptophan in the protein.

Figure 8 compares the fluorescence emission spectra of both wild-type and Y125W/Y133F/Y136F α-synuclein at the same concentrations in the region where both tyrosine and tryptophan emission is observed. Excitation of 265 nm (Figure 8(a)) was used to specifically excite tyrosine and excitation of 290 nm was used to specifically excite tryptophan (Figure 8(b)). The emission spectrum of wild-type α-synuclein excited at 265 nm shows tyrosine emission at 304 nm corresponding to the four tyrosine residues present and a low level of emission in the vicinity of 355 nm where Trp would emit (due to the "tail" of the Tyr emission). Excitation of wild-type α-synuclein at 290 nm shows negligible emission at 355 nm, consistent with the lack of Trp. Y125W/Y133F/Y136F α-synuclein excited at these two wavelengths shows major peaks centered at 355 nm for the tryptophan emission. The intensity of the tryptophan emission with excitation at 265 nm is

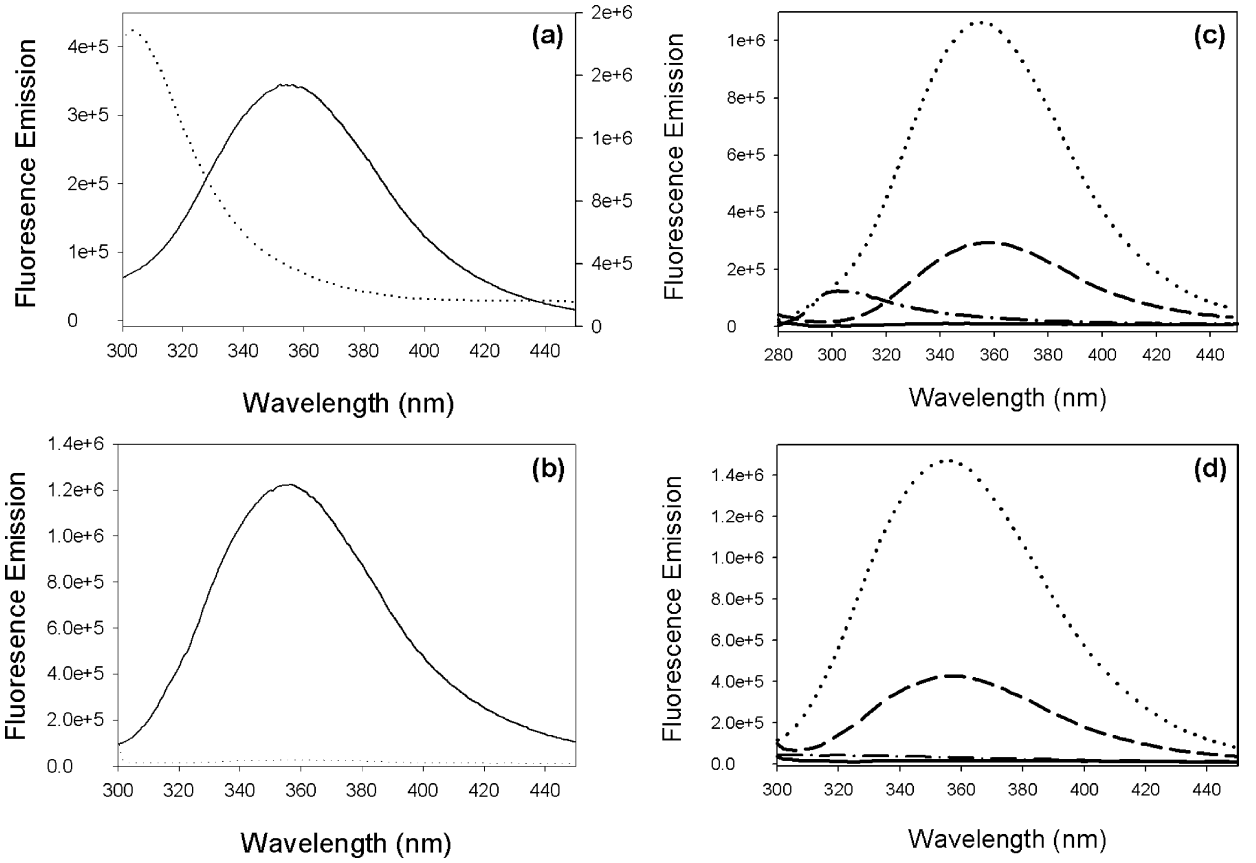

Figure 8. Fluorescence resonance energy transfer in monomeric Y125W/Y133F/Y136F α-synuclein. Fluorescence emission of wild-type (dotted) and Y125W/Y133F/Y136F (continuous line) α-synuclein with excitation at (a) 265 nm and (b) 290 nm. (a) Only Tyr emission from the wild-type and essentially only Trp emission from the mutant; (b) the reverse, namely only Trp emission from the mutant and no emission from the wild-type. (c) and (d) A comparison of the nitrated and non-nitrated forms of WT (dot-dash line and continuous line, respectively) and Y125W/Y133F/Y136F (dotted line and broken line, respectively) α-synuclein. Nitration of α-synuclein quenches its Tyr fluorescence. (c) Excitation at 265 nm; (d) excitation at 290 nm. The nitrated wild-type α-synuclein shows no tyrosine emission maximum, indicating that the tyrosine residues have been nitrated. The nitrated Y125W/Y133F/Y136F α-synuclein shows significantly reduced tryptophan emission at both excitation wavelengths, confirming energy transfer between Tyr39 and Trp125 in the non-nitrated samples.

comparable to that with excitation at 290 nm, indicating substantial energy transfer. No emission maximum for tyrosine is detectable with excitation at 265 nm of Y125W/Y133F/Y136F α-synuclein, due to the fluorescence energy transfer to Trp.

To further check for the presence of energy transfer, both proteins were nitrated, since nitration of tyrosine quenches its fluorescence, and would thus destroy any FRET. The emission spectra of nitrated wild-type α-synuclein show no tyrosine emission maxima (Figure 8(c) and (d)), indicating that the tyrosine residues have been nitrated. Emission spectra of the nitrated Y125W/Y133F/Y136F α-synuclein show significantly reduced tryptophan emission at both excitation wavelengths. This confirms the presence of energy transfer between Tyr39 and Trp125 in the non-nitrated samples.

Energy transfer in the fibrils during fibrillation was monitored by collecting fluorescence emission spectra of the resuspended sampled pellet fractions taken during the incubation of Y125W/Y133F/Y136F α-synuclein and exciting at 265 nm (all pellet resuspensions were clear). Figure 9 shows the emission spectra produced during the incubation. Increases in the tryptophan emission parallel the ThT fibrillation curve (Figure 9, inset). Normalization of the pellet fraction emission spectra for concentration shows no significant changes in the emission intensity (data not shown). Thus, energy transfer in the fibrils remains constant, and the increased signal with increased incubation time reflects the increasing concentration of fibrils.

Energy transfer in the supernatant fractions was observed by collecting fluorescence emission spectra of the supernatant fractions in the same way as for the pellets described above. Figure 10(a) shows the emission spectra from excitation at 265 nm of the supernatant fractions. FRET emission intensities increase during the first 30 h of incubation then start to drop as fibril formation begins. Comparison of emission intensity at 355 nm to the ThT fluorescence (Figure 10(a), inset) shows

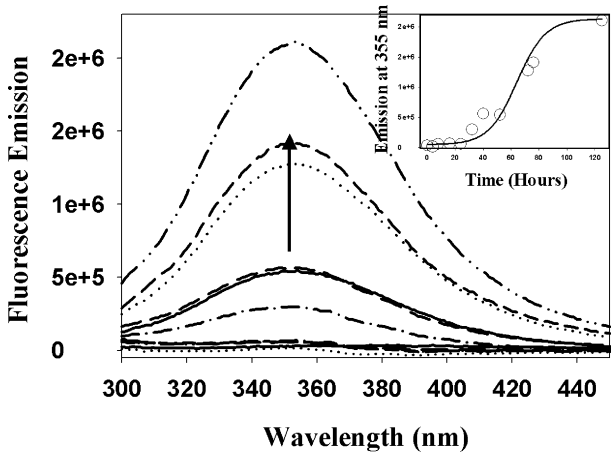

Figure 9. FRET spectra of pellet samples taken during the fibrillation of Y125W/Y133F/Y136F α-synuclein. The spectra show Trp emission fluorescence when Tyr39 is excited at 265 nm. The inset shows the emission intensity at 355 nm *versus* time (circles) compared to the ThT fluorescence signal (continuous line). Samples were prepared as described for Figure 3.

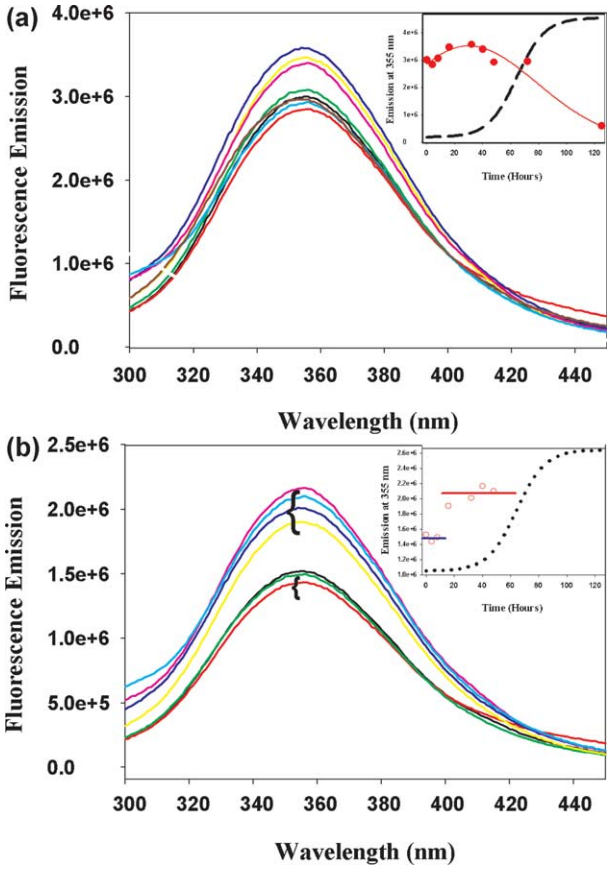

Figure 10. FRET spectra of supernatant samples during the fibrillation of Y125W/Y133F/Y136F α-synuclein. (a) Trp emission when Tyr9 is excited at 265 nm. The inset shows the emission intensity at 355 nm *versus* time (continuous line with filled circles) compared to the ThT fluorescence signal (broken line). (b) Concentration-normalized spectra for the energy transfer contribution to the fluorescence. The spectra cluster into two groups, one with lower intensity, similar to that of the monomer, the other with higher intensity, corresponding to the early oligomeric intermediate. The inset shows the normalized emission intensity at 355 nm *versus* time (red continuous lines with open circles) compared to the ThT fluorescence (broken line). The data cluster into two groups, corresponding to monomer and early oligomer. Samples were prepared as described for Figure 3.

that the changes in FRET correspond predominantly to the formation and decay of the early oligomeric intermediate. Normalization of the emission spectra for concentration (Figure 10(b)) shows that the emission intensities remain similar during the first 12 h, corresponding to the monomer. After this time, there is a jump in the emission intensities as a newer population arises with a different Tyr to Trp distance. This population (the early oligomeric intermediate) shows relatively constant emission intensity (when concentration-normalized) for the remainder of the lag time and the start of the elongation phase (Figure 10(b), inset).

Thus, the first 12 h of incubation are dominated by the unfolded monomer; by the middle of the lag phase there is a jump in the energy transfer efficiency as a new population dominates with a closer proximity for the two fluorophores. This species, the early oligomeric species, dominates for the remainder of the lag time and the start of the elongation phase. These initial oligomers are unstable, however, and eventually undergo conversion, directly or indirectly, to fibrils. For the late oligomeric species, there is a further small increase in energy transfer, which is apparent when the spectra are concentration-normalized (data not shown).

Fibrillation, based on ThT fluorescence, is complete by 80 h (Figures 1 and 4), however, at significantly longer times ($\geq$125 h) there is a decrease in energy transfer, concomitant with the appearance of a new emission maximum around 304 nm at 125 h. The emission maximum at 304 nm corresponds to Tyr emission, which indicates the loss of energy transfer to tryptophan. As will be shown subsequently, this arises from the formation of dityrosine.

Figure 11 shows a comparison of the FRET emission spectra (excitation at 265 nm) for the four distinctive populations observed during the fibrillation of Y125W/Y133F/Y136F α-synuclein; namely, the monomer, early and late oligomers and fibrils, normalized for protein concentration. The spectra show a broad tryptophan emission centered at 355 nm. Comparison of the different intensities reflects the relative distances between Tyr39 and Trp125 in these populations. The spectra show an increase in energy transfer going from the monomer to the early oligomeric intermediate, and to the late oligomeric intermediate, indicating a decrease in the distance between tyrosine and tryptophan, and thus a more compact structure in the oligomeric

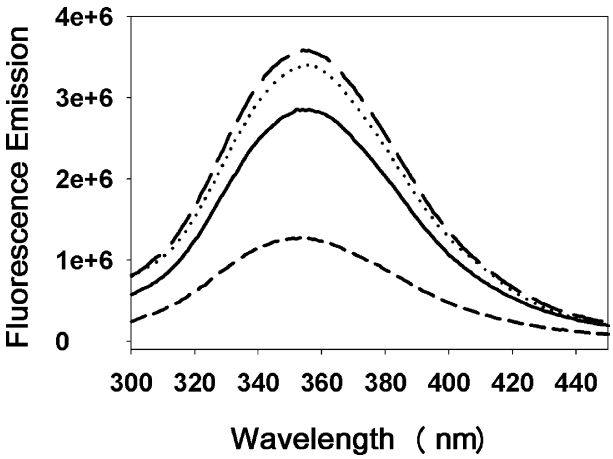

Figure 11. FRET spectra of the key species in the fibrillation of Y125W/Y133F/Y136F α-synuclein. Tyr39 was excited at 265 nm, and the emission at 355 nm arises from fluorescence energy transfer to Trp125, with the exception of the fibrils (broken line), which is not due to energy transfer, but reflects the small amount of Trp emission due to excitation of Trp at 265 nm. The spectra are concentration-normalized. Samples were prepared as described for Figure 3. Line codes: monomer (continuous, time zero), early oligomeric intermediate (dotted, 32 h), fibrils (broken, 125 h), and late soluble oligomers (dot-dash, 76 h).

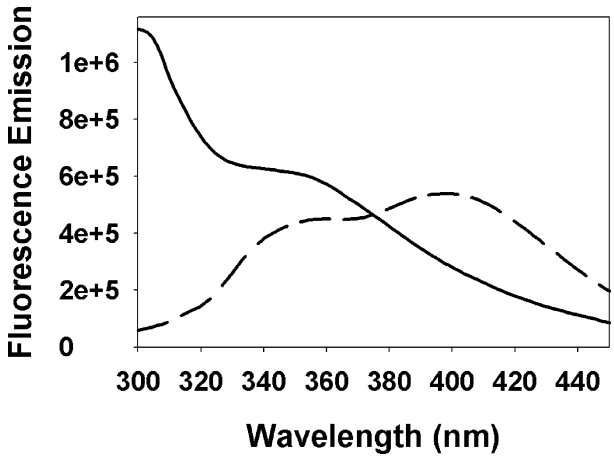

Figure 12. The formation of dityrosine at long incubation times. Fluorescence emission spectra of Y125W/Y133F/Y136F α-synuclein at 265 nm excitation (continuous line) and 290 nm excitation (broken line) for the 125 h supernatant sample showing dityrosine formation by the 410 nm maxima when excited at 290 nm, and the enhanced 304 nm maxima due to Tyr, when excited at 265 nm. The sample was prepared as described for Figure 3.

intermediates during the lag time and elongation. The spectrum for the fibrils shows no energy transfer (the spectrum for the fibrils (broken line in Figure 11) is not due to energy transfer, but reflects the small amount of Trp emission due to excitation of Trp at 265 nm), which could either reflect quenching of Tyr or Trp in the fibrils, or a very long distance between the Tyr and Trp. Since no tyrosine emission is observed for fibrils, it is most likely that the fibril structure itself is quenching the tyrosine emission.

Examination of the supernatant fractions for Y125W/Y133F/Y136F α-synuclein incubated for times longer than 125 h revealed the same unusual emission spectra as that at 125 h. Figure 12 shows the emission spectra for the 125 h supernatant fraction with excitation at 265 nm and at 290 nm. The emission spectrum at 265 nm excitation shows the loss of energy transfer by the tyrosine emission maxima around 300 nm and lower tryptophan emission at 355 nm. The surprising aspect of the tyrosine emission is how enhanced the intensity is compared to the tryptophan emission. A clue as to what may be causing this enhanced emission is shown in the 290 nm excitation spectrum: whereas there is a maximum for the tryptophan at 355 nm, the tyrosine emission has shifted to 402 nm. This is characteristic of the emission maximum of dityrosine.[20] The excitation maximum for dityrosine is around 310 nm, so significant excitation will arise from excitation at 290 nm. Dityrosine arises from oxidation and is produced by covalent bond formation between two Tyr sidechains involving tyrosyl radicals. In this case, the dityrosine formation must be intermolecular, since only one tyrosine residue (Tyr39) is present per protein molecule in Y125W/Y133F/Y136F. No dityrosine fluorescence emission was observed in the fibrils at any time. An EM image of the late supernatant sample showed only amorphous deposits.

Förster distance measurements in Y125W/Y133F/Y136F

Y125W/Y133F/Y136F α-synuclein was shown (see above) to exhibit energy transfer between Tyr39 and Trp125. We calculated the Förster critical distance, R_o to be 1.5×10^{-7} cm (15 Å). This means tyrosine and tryptophan distances can be calculated reliably between 10 Å and 30 Å under our experimental conditions. In order to calculate these distances, the efficiency of energy transfer, E, must be found experimentally. Many methods of finding energy transfer efficiency have been reported.[21] Typically, it is necessary to measure the emission of the donor in the presence and in the absence of the acceptor. Although the intrinsic properties of tyrosine and tryptophan fluorescence make it difficult to obtain intensity values for the donor without deconvolution, it has been shown that efficiency measurements can be made using fluorescence excitation spectra to monitor the acceptor emission intensity.[22] The efficiency of energy transfer in our experiments was found by measuring excitation spectra for the mutants Y125W/Y133F/Y136F and Y39F/Y125W/Y133F/Y136F.

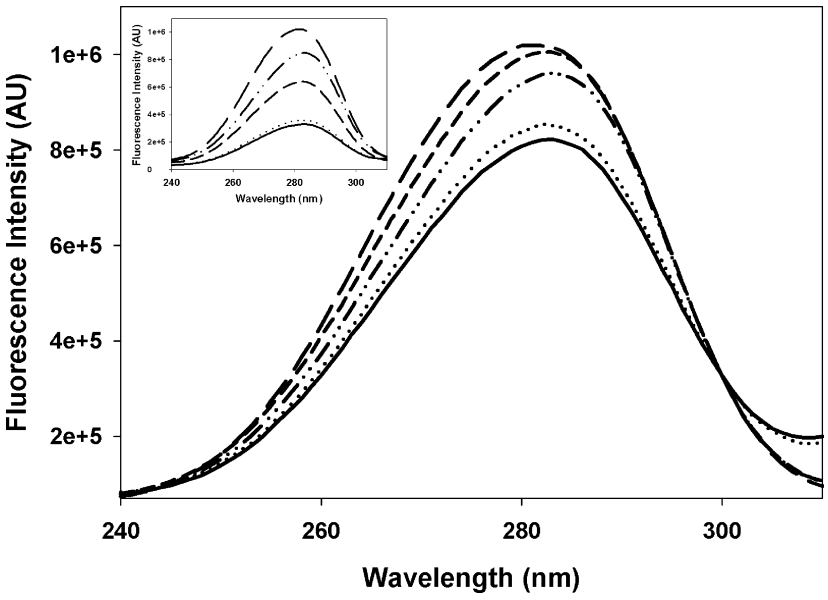

Figure 13. Fluorescence excitation spectra of key species during the fibrillation of Y125W/Y133F/Y136F α-synuclein. The excitation spectra were compared to that of Y39F/Y125W/Y133F/Y136F α-synuclein (no Tyr) by normalization at 300 nm. The greater the intensities, the greater the energy transfer present. The inset shows the non-normalized spectra. Samples were prepared as described for Figure 3. Emission was at 340 nm. Line codes: monomeric Y125W/Y133F/Y136F (dot-dash, time zero), monomeric Y39F/Y125W/Y133F/Y136F (continuous, 0 h), early oligomeric Y125W/Y133F/Y136F (short dash, 32 h), fibrillar Y125W/Y133F/Y136F (dotted, 125 h), and late oligomeric Y125W/Y133F/Y136F (long dash, 76 h).

The Y39F/Y125W/Y133F/Y136F α-synuclein excitation spectrum shows just tryptophan emission, since it lacks the tyrosine residue at position 39. The absorbance spectrum of Y125W/Y133F/Y136F provided the total amount of photon energy absorbed. Thus, the difference in the tryptophan emission intensities for these two mutants was used to find the efficiency when compared to the absorption spectra.

Figure 13 shows the fluorescence excitation spectra of Y39F/Y125W/Y133F/Y136F α-synuclein compared to the fluorescence excitation spectra of samples taken during the incubation of Y125W/Y133F/Y136F. All spectra were collected at the same concentration of protein (20.0 μM). The spectra were recorded at an emission wavelength of 340 nm, where fluorescence originates exclusively from tryptophan. All spectra were then normalized for intensity at 300 nm, where only tryptophan can be excited. The larger the intensity of the tryptophan excitation, the more energy transfer is occurring and hence the closer the tyrosine and tryptophan residues are to each other. As was seen in the emission spectra, there is an increase in energy transfer from the start of fibrillation to the end of the elongation phase in the supernatant species. Calculation of the distances using Förster theory shows the distance in the starting monomer, early oligomeric intermediate, and late oligomeric species to be 24.9(±1.8) Å, 21.9(±1.2) Å, and 18.8(±1.3) Å, respectively. Samples of fibrillar Y125W/Y133F/Y136F α-synuclein show no measurable energy transfer and virtually overlap the Y39F/Y125W/Y133F/Y136F spectra. This indicates the lack of energy transfer, which could arise from two sources; either the distance between the Tyr and Trp residues becomes so great that no transfer occurs, or one or both fluorescence residues becomes quenched in the fibrils. As noted, the lack of Tyr emission in the fibrils suggests that Tyr39 is quenched in the fibrils, which would indicate that it is at least partially buried in the fibrils.

Discussion

Mutants and wild-type α-synuclein have similar fibrillation properties

The work described here provides insight into the structural changes occurring during the aggregation and fibrillation of α-synuclein, a protein whose aggregation has been linked to Parkinson's disease.[6,7] The four tyrosine residues of wild-type α-synuclein at positions 39, 125, 133, and 136 provide optimal sites for the introduction of other naturally occurring amino acids such as phenylalanine and tryptophan, which have properties similar to those of tyrosine. Replacement of these tyrosine residues in α-synuclein with phenylalanine or tryptophan introduces new fluorescent properties to the protein. Both Y125W/Y133F/Y136F (one Tyr at position 39) and its homolog Y39F/Y125W/Y133F/Y136F (no Tyr) have physical properties similar to those of wild-type α-synuclein, including the ability to form fibrils, similar fibrillation kinetics, and fibril morphology. The small differences in the lag time and elongation rates for fibrillation can be explained by the increased hydrophobicity of the mutants accelerating the nucleation step of fibrillation and decreasing the rate of fibril extension, perhaps by affecting the surface hydrophobicity of the key amyloidogenic partially folded intermediate (see Scheme 1). Thus, these mutations introduce new amino acids into the protein without greatly altering its aggregation properties.

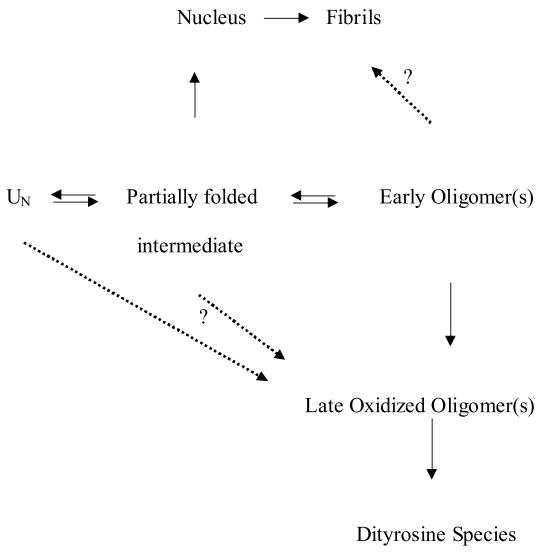

Scheme 1.

α-Synuclein forms a metastable early oligomeric intermediate

The structural characterization of samples removed at various time-points during the incubation of Y125W/Y133F/Y136F reveals structural similarities to previous biophysical studies for wild-type α-synuclein. In particular, structural changes are observed that correspond to formation of a transient oligomeric intermediate: confirmation that this intermediate is oligomeric comes from dynamic light-scattering experiments (Figure 6). Multiple oligomeric protofibrillar species have been reported for α-synuclein and two mutants associated with familial Parkinson's disease.[13]

Scheme 1 shows the proposed aggregation pathways for α-synuclein based, in part, on previous research,[12,23] as well as the results from the current study of Y125W/Y133F/Y136F.

The monomeric population at the start of fibrillation is intrinsically unfolded (U_N). This conformation is in equilibrium with the critical amyloidogenic, partially folded intermediate. Detectable structural changes start to occur after the first 8–10 h at pH 7.5 and 100 mM NaCl. The supernatant shows an increase in β-structure, with the maximum amount of β-structure being reached by the end of the lag phase (about 40 h) and then a subsequent decrease in this population during the elongation phase. The major population present at this time is the early oligomeric intermediate, which has significant β-structure (from FTIR data), hydrophobic patches (based on ANS binding) and a compact, partially folded subunit structure (from the FRET and CD data). This oligomeric intermediate is assumed to form from the association of the amyloidogenic partially folded intermediate, at a slightly faster rate than that of nucleation to give fibrils. The FTIR and CD data suggest that there is more than one form of the early oligomeric intermediate.

The decrease in the early oligomer population as fibril growth begins is reflected by a decrease in the concentration of protein in the supernatant, and corresponds to the intermediate becoming a source of protein for fibril growth when the monomer population is exhausted (Scheme 1). There are two most likely ways in which this could happen: the early oligomeric intermediates could transform directly into fibrillar material, or they could dissociate into monomeric species that add to growing fibrils. The present data do not allow us to discriminate between these two possibilities.

The other notable observation concerns the presence of significant soluble protein in the supernatant after fibrillation has ceased. On the basis of the results of experiments to be reported elsewhere, at least some of this soluble material consists of oligomers of Met-oxidized α-synuclein (as determined by mass spectrometry). We have shown that oxidation of the Met residues in α-synuclein to the corresponding sulfoxides leads to the formation of soluble oligomers that are stable and do not form fibrils.[23] The mechanism for Met oxidation would be *via* H_2O_2 generation due to trace contamination of α-synuclein by tightly bound iron.[24,25] As shown in Scheme 1, the Met-oxidized α-synuclein oligomers must arise from soluble monomer or oligomers, since no oxidation of α-synuclein in the fibrils is observed. The fact that accelerating the rate of fibrillation by increasing the concentration of salt leads to decreased concentration of late soluble oligomers is consistent with decreased oxidation of Met due to the shorter lifetimes of the soluble α-synuclein. The Met-oxidized α-synuclein oligomers are stable and do not form fibrils.[23,26–28] The remainder of the soluble late oligomer probably arises from association of the amyloidogenic partially folded intermediate into stable "misfolded" oligomers that do not dissociate or rearrange to form fibrils.

Observation of energy transfer in the supernatant during fibrillation further supports Scheme 1. The first 10 h of fibrillation in 100 mM NaCl are dominated by unfolded monomeric species. By the middle of the lag phase, however, there is a reduction of the distance between Tyr39 and Trp125 as a new population, the early oligomeric intermediate, dominates with a closer proximity for the two fluorophores. The 3 Å decrease in distance between Tyr39 and Trp125 in the early oligomer can be compared to the overall Stokes radius of 27 Å for the monomer, and 20 Å for the amyloidogenic partially folded intermediate, and corresponds to a 13% decrease in distance between Tyr39 and Trp125.[12] In the late oligomeric species, the energy transfer results indicate that the Tyr and Trp have become 6 Å closer than in the monomer. It has been proposed that oligomeric species formed during the aggregation of α-synuclein might be more toxic than fibrils in Parkinson's disease.[29,30] Thus, either

or both the early and late oligomers might be cytotoxic.

The C-terminal region of α-synuclein is solvent-exposed in all aggregation species and fibrils

Y125W/Y133F/Y136F α-synuclein has a single tryptophan residue located at position 125 in the acidic C-terminal domain of the protein. The wavelength maximum for tryptophan emission can be used to study changes in the solvent exposure of Trp125 during aggregation. Surprisingly, since tryptophan is a hydrophobic amino acid, the Trp125 emission indicates the residue is solvent-exposed during the entire aggregation process.

For the pelleted samples of Y125W/Y133F/Y136F, the emission wavelength maximum remains constant at 352 nm for the duration of fibrillation. This indicates that Trp125 is either solvent-exposed on the surface of the fibril core or, more likely, in a region of polypeptide (the C-terminal tail), that is not incorporated into the fibril core. In the supernatant samples, the tryptophan residue also remains solvent-exposed, based on the fluorescence emission, which is blue-shifted from 356($\pm$2) nm in the monomer and early oligomer to 352($\pm$1) nm in the late oligomer. What would cause this hydrophobic amino acid to remain solvent-exposed during aggregation? The answer probably lies in the highly acidic amino acid composition of the C-terminal region, which is predicted to lack ordered secondary structure. The intrinsic tryptophan fluorescence of the mutants Y133W and Y136W where the Trp residue is also located in the C-terminal region has been examined (N.B. *et al*., unpublished results). These mutants show the same solvent-exposed emission for the tryptophan residue at positions 133 and 136 as is exhibited at 125. Clearly, the C-terminal region of α-synuclein remains solvent-exposed in all the species present during fibrillation.

The N-terminal region of α-synuclein is part of the fibril core

Energy transfer in Y125W/Y133F/Y136F α-synuclein allows measurement of the distance between the N-terminal repeat domain and the acidic C-terminal region. Experiments to measure the Förster distance in fibrils revealed that energy transfer was not detectable in fibrils. The excitation spectrum for fibrillar Y125W/Y133F/Y136F α-synuclein virtually overlaps the spectrum for Y39F/Y125W/Y133F/Y136F α-synuclein, a homolog lacking tyrosine and thus having no energy transfer. Since excitation of fibrils at 265 nm does not show tyrosine emission, it is logical to assume that Tyr39 is buried in the fibril structure and its fluorescence is quenched. Consistent with this is the observation that the intrinsic tryptophan fluorescence of the Y39W mutant reveals that position 39 is solvent-exposed in the soluble oligomers but is much less solvent-exposed in the fibrils (A. Dusa *et al*., unpublished results).

Formation of dityrosine

Y125W/Y133F/Y136F α-synuclein has a single tyrosine residue located at position 39 in the N-terminal amphipathic repeat region of the protein. Dityrosine formation was observed in the soluble late oligomers in the supernatant at 125 h and longer (long after the completion of fibrillation). Since Y125W/Y133F/Y136F has only one tyrosine residue, the covalent cross-linking must be intermolecular. Dityrosine formation was never observed in the pelleted fibril samples. Since the dityrosine fluorescence signal appears only after fibrillation is complete, it would seem most likely that it arises from the late oligomers. This suggests that the two Tyr39 residues are in, or can come into, close proximity in the non-fibrillating late oligomeric species and that the tyrosine residues must be solvent-exposed in order to undergo oxidation. This observation suggests that the formation of dityrosine dimers does not accelerate fibrillation of α-synuclein as has been suggested.[31] On the other hand, it does explain the observation of stable, non-fibrillar aggregates containing dityrosine.[32]

α-Synuclein aggregation is determined by competing kinetic pathways

The ease with which monomeric α-synuclein is transformed into highly ordered fibril structures reflects the initial intrinsically disordered state, which readily permits the flexibility for the polypeptide chain to undergo the necessary topological rearrangements for association between molecules. As shown in Scheme 1, the aggregation of α-synuclein is complex; in fact, this scheme is a simplification, because there appear to be at least two or three different forms of the early oligomeric intermediate and possibly multiple forms of the late oligomer as well. Thus, the final products are determined by the outcome of competing pathways at several stages, especially for the critical partially folded intermediate.

Materials and Methods

Materials

Thioflavin (ThT) and 1-anilinonaphthalene-8-sulfonic acid (ANS) were obtained from Sigma-Aldrich. All other chemicals were analytical grade and obtained from Fisher Chemicals or VWR Scientific.

Site-directed mutagenesis of human α-synuclein

Wild-type α-synuclein and its mutants were expressed in *Escherichia coli* BL21(DE3) Gold cell line transfected with pRK172/human α-synuclein plasmid containing the gene for carbenicillin resistance.[23] The mutants

Y125W/Y133F/Y136F and Y39F/Y125W/Y133F/Y136F were created using the QuikChange method (Stratagen, La Jolla, CA).

Expression and purification of α-synuclein and mutants

Expression and purification of human recombinant α-synuclein and its mutants were performed as described.[23] Electrospray mass spectroscopy (see below) was used to verify the molecular masses and purity of the proteins after expression (Table 1). Purified protein was lyophilized and stored at −80 °C. To prepare protein samples for use in experiments, the protein was dissolved in sterile H_2O/NaOH (pH 11.0) for 20 min on ice then neutralized to pH 7.5, and ultracentrifuged at 100,000 rpm for 10 min using a Beckman Airfuge to pellet any insoluble material. Protein concentration was determined spectrophotometrically as described below.

UV-visible spectrophotometry

The absorbance of proteins for concentration determination and other calculations was measured using a UV-2401 PC spectrophotometer (Shimadzu, Japan). Extinction coefficients used were $\varepsilon_{276\ nm}=0.401$, 0.474, and 0.374 mg/ml for wild-type, Y125W/Y133F/Y136F and Y39F/Y125W/Y133F/Y136F α-synuclein, respectively.

Mass spectrometry (MS)

A MicroMass Quattro II electrospray mass spectrometer was used to obtain mass spectra. Samples for MS analysis were made by preparing 2 ml of 10 μM protein in 50% (v/v) aqueous acetonitrile. Samples were adjusted to pH 2.0 with 12 M HCl immediately before use. Injection was carried out using a syringe pump (Harvard Apparatus, Holliston, MA) at a flow-rate of 6 μl/min. The source temperature was set to 90 °C, the capillary voltage was 3.0 kV, and electrospray positive ionization mode was used.

Thioflavin T fibrillation assay

Measurement of fibrillation kinetics was carried out by monitoring fluorescence during protein fibrillation in the presence of ThT, which shows increased fluorescence when binding to amyloid fibrils.[33,34] The fluorescence was monitored using an excitation of 450 nm and measuring the emission at 485 nm. Samples were prepared containing 1 mg/ml of protein, 100 mM NaCl, 20 mM sodium phosphate buffer (pH 7.5), 20 μM ThT. Multiple samples were assayed by taking 100 μl of the mixture and pipetting it into eight to ten wells on a 96-well plate (white plastic, clear bottom). A Teflon bead (1/8 in diameter (1 in ~2.54 cm); McMaster-Carr, Los Angeles, CA) was added to each well. Plates were then sealed and monitored with a fluorescence plate reader (Fluoroskan Ascent) at 37 °C and shaking at 600 rpm (diameter 2 mm). For kinetic analysis, the ThT fluorescence intensity *versus* time was fit to a sigmoidal curve as described.[35]

Preparation of pellet and supernatant samples

When aliquots of fibrillation incubation at selected times were needed, samples were prepared by using volumes of 4 ml of incubation sample of 2 mg/ml of protein, 20 mM sodium phosphate buffer (pH 7.5), 100 mM NaCl, and stirring in 10 ml vials. For supernatant and pellet samples, 200 μl aliquots were removed and centrifuged at 14,000 rpm for 45 min in an Eppendorf microfuge. The supernatant was removed for analysis. The pellet was washed once in the same buffer and then resuspended in the volume of buffer removed for analysis.

Electron microscopy

Electron microscopy (EM) images of fibrils were obtained using a JEOL JEM-100B transmission electron microscope operating with an accelerating voltage of 80 kV. Samples were prepared on carbon-coated pioloform copper grids by negative staining with 1% (w/v) uranyl acetate.

ATR-FTIR spectroscopy

ATR-FTIR spectra were recorded on a ThermoNicolet Nexus 670 FTIR spectrometer equipped with an MCT detector. The samples were prepared as hydrated thin films as described,[16,36] on the surface of an out-of-compartment germanium trapezoidal internal reflectance element (IRE). Then 512 interferograms were co-added at 1 cm^{-1} resolution to generate each spectrum. Spectra were deconvoluted to ascertain the percentage of secondary structure using the program GRAMS32 (Galactic Industries). FSD and second derivatives were used to deconvolve the spectra. Peak positions identified by both were used for the curve-fitting routine. In curve-fitting, the initial peak positions found were fixed and the peak width was allowed to vary from 15 cm^{-1} to 30 cm^{-1}. Peak height, width, and percentage Lorentzian were allowed to vary until the solution converged to a minimum, at which time the constraint on the peak positions was removed and curve-fitting continued until the minimum was reached. Percentage secondary structure peak assignments were made as published.[16,17]

Samples were prepared by taking aliquots out of a bulk mixture allowed to incubate at 37 °C in 20 mM PBS (pH 7.5), 100 mM NaCl, and 2 mg/ml of protein with stirring. Aliquots were centrifuged to separate pellet and supernatant. Pellets were resuspended in the same volume as the removed supernatant using 20 mM PBS (pH 7.5), 100 mM NaCl.

Fluorescence spectroscopy

Fluorescence excitation and emission spectra were taken using a FluoroMax-2 spectrofluorometer (Instruments S.A., Inc., Jobin Yvon-Spex). Samples were diluted to a concentration of approximately 20 μM in 1 ml. Quartz cuvettes (Hellma) were used with a sample volume of either 1 ml or 20 μl.

Nitration of α-synuclein

Nitrated α-synuclein was prepared as described.[23,37] The presence of nitrotyrosine was detected using UV–Vis spectroscopy and mass spectrometry.

Förster distance calculations

Förster theory allows the determination of the distance between two chromophores within a protein.[19] Tyrosine and tryptophan are two such chromophores, with tyrosine acting as the donor and tryptophan acting as the acceptor. The Y125W/Y133F/Y136F α-synuclein

mutant was designed to take advantage of Förster theory, and meets all the requirements set forth by the theory for energy transfer to occur. The α-synuclein mutant Y39F/Y125W/Y133F/Y136F was designed not to have Tyr-Trp energy transfer, lacking tyrosine at position 39, and serves as a standard for pure acceptor fluorescence. Förster theory is represented by the following equation:

$$R = ((1/E)-1)^{1/6}R_0$$

where R is the distance between chromophores, E is the efficiency of energy transfer, and R_0 is the Förster critical distance. The Förster critical distance corresponds to the distance at which 50% of the absorbed energy is transferred from the donor to the acceptor. The efficiency of energy transfer can be found experimentally, and the Förster critical distance can be calculated using the following equation:

$$R_0 = [8.79 \times 10^{-25}(k^2/n^4)\Phi_D J_{AD}]^{1/6}$$

k^2 is the orientation factor and is equal to 2/3 for a random orientation. The refractive index of the solvent, n, is 1.334 for phosphate buffer. The fluorescence quantum efficiency of the donor represented by Φ_D is equal to 0.14 for tyrosine. Finally, the spectral overlap integral between the donor and acceptor, J_{AD}, is equal to $4.8\times 10^{-16}\,M^{-1}\,cm^6$ for the tyrosine/tryptophan pair. Therefore, the Förster critical distance is calculated to be 1.5×10^{-7} cm for energy transfer between tyrosine and tryptophan for these experiments.[38]

The efficiency of energy transfer, E, can be found experimentally using the following equation:

$$E = (I - I_A)/A_D$$

where I is the fluorescence intensity of the acceptor in the presence of the donor, I_A is the fluorescence intensity of the acceptor in the absence of the donor, and A_D is the absorbance of the acceptor in the presence of the donor. Such being the case, the Y125W/Y133F/Y136F α-synuclein mutant can be used to find I and A_D, and the Y39F/Y125W/Y133F/Y136F α-synuclein mutant can be used to find I_A. All values used were at 280 nm.

Fluorescence excitation spectra were obtained of both Y125W/Y133F/Y136F and Y39F/Y125W/Y133F/Y136F using an emission wavelength of 340 nm scanning the region from 240–310 nm. From the excitation spectra, I_{280} can be found for both mutants. All samples were prepared for both mutants at identical concentrations (20 μM). Normalization was carried out by making the fluorescence and absorbance intensities equal at 300 nm, since tyrosine does not absorb at 300 nm and all the fluorescence comes from tryptophan.

Acknowledgements

We thank Volodya Uversky, Atta Ahmed, and John Goers for their contributions, and Jonathan Krupp for help with electron microscopy imaging and editing. This research was supported by grant NS 43778 from The National Institutes of Health (to A.L.F.).

References

1. Galvin, J. E., Lee, V. M., Schmidt, M. L., Tu, P. H., Iwatsubo, T. & Trojanowski, J. Q. (1999). Pathobiology of the Lewy body. *Advan. Neurol.* **80**, 313–324.
2. Polymeropoulos, M. H., Lavedan, C., Leroy, E., Ide, S. E., Dehejia, A., Dutra, A. *et al*. (1997). Mutation in the alpha-synuclein gene identified in families with Parkinson's disease. *Science*, **276**, 2045–2047.
3. Kruger, R., Kuhn, W., Muller, T., Woitalla, D., Graeber, M., Kosel, S. *et al*. (1998). Ala30Pro mutation in the gene encoding alpha-synuclein in Parkinson's disease. *Nature Genet.* **18**, 106–108.
4. Uversky, V. N., Li, J. & Fink, A. L. (2001). Pesticides directly accelerate the rate of alpha-synuclein fibril formation: a possible factor in Parkinson's disease. *FEBS Letters*, **500**, 105–108.
5. Di Monte, D. A., Lavasani, M. & Manning-Bog, A. B. (2002). Environmental factors in Parkinson's disease. *Neurotoxicology*, **23**, 487–502.
6. Spillantini, M. G., Schmidt, M. L., Lee, V. M., Trojanowski, J. Q., Jakes, R. & Goedert, M. (1997). Alpha-synuclein in Lewy bodies. *Nature*, **388**, 839–840.
7. Spillantini, M. G., Crowther, R. A., Jakes, R., Hasegawa, M. & Goedert, M. (1998). Alpha-synuclein in filamentous inclusions of Lewy bodies from Parkinson's disease and dementia with lewy bodies. *Proc. Natl Acad. Sci. USA*, **95**, 6469–6473.
8. Masliah, E., Rockenstein, E., Veinbergs, I., Mallory, M., Hashimoto, M., Takeda, A. *et al*. (2000). Dopaminergic loss and inclusion body formation in alpha-synuclein mice: implications for neurodegenerative disorders. *Science*, **287**, 1265–1269.
9. Feany, M. B. & Bender, W. W. (2000). A Drosophila model of Parkinson's disease. *Nature*, **404**, 394–398.
10. Jakes, R., Spillantini, M. G. & Goedert, M. (1994). Identification of two distinct synucleins from human brain. *FEBS Letters*, **345**, 27–32.
11. Goedert, M. (1997). Familial Parkinson's disease. The awakening of alpha-synuclein. *Nature*, **388**, 232–233.
12. Uversky, V. N., Li, J. & Fink, A. L. (2001). Evidence for a partially folded intermediate in alpha-synuclein fibril formation. *J. Biol. Chem.* **276**, 10737–10744.
13. Lashuel, H. A., Petre, B. M., Wall, J., Simon, M., Nowak, R. J., Walz, T. & Lansbury, P. T., Jr (2002). Alpha-synuclein, especially the Parkinson's disease-associated mutants, forms pore-like annular and tubular protofibrils. *J. Mol. Biol.* **322**, 1089–1102.
14. Volles, M. J. & Lansbury, P. T., Jr (2003). Zeroing in on the pathogenic form of alpha-synuclein and its mechanism of neurotoxicity in Parkinson's disease. *Biochemistry*, **42**, 7871–7878.
15. Uversky, V. N., Li, J., Souillac, P. O., Millett, I. S., Doniach, S., Jakes, R. *et al*. (2002). Biophysical properties of the synucleins and their propensities to fibrillate: inhibition of alpha-synuclein assembly by beta- and gamma-synucleins. *J. Biol. Chem.* **277**, 11970–11978.
16. Oberg, K. A. & Fink, A. L. (1998). A new attenuated total reflectance Fourier transform infrared spectroscopy method for the study of proteins in solution. *Anal. Biochem.* **256**, 92–106.
17. Seshadri, S., Khurana, R. & Fink, A. L. (1999). Fourier transform infrared spectroscopy in analysis of protein deposits. *Methods Enzymol.* **309**, 559–576.
18. Fink, A. L. (1999). ANS. In *The Encyclopedia of Molecular Biology* (Creighton, T. E., ed.), pp. 140–142, Wiley, New York.

19. Forster, T. (1948). Zwischenmoleculare energiewanderung und fluoreszenz. *Ann. Der Phys.* **2**, 55–75.
20. Heinecke, J. W., Li, W., Daehnke, H. L., III & Goldstein, J. A. (1993). Dityrosine, a specific marker of oxidation, is synthesized by the myeloperoxidase–hydrogen peroxide system of human neutrophils and macrophages. *J. Biol. Chem.* **268**, 4069–4077.
21. Berney, C. & Danuser, G. (2003). FRET or no FRET: a quantitative comparison. *Biophys. J.* **84**, 3992–4010.
22. Eisenhawer, M., Cattarinussi, S., Kuhn, A. & Vogel, H. (2001). Fluorescence resonance energy transfer shows a close helix-helix distance in the transmembrane M13 procoat protein. *Biochemistry*, **40**, 12321–12328.
23. Uversky, V. N., Yamin, G., Souillac, P. O., Goers, J., Glaser, C. B. & Fink, A. L. (2002). Methionine oxidation inhibits fibrillation of human alpha-synuclein *in vitro*. *FEBS Letters*, **517**, 239–244.
24. Tabner, B. J., Turnbull, S., El Agnaf, O. M. & Allsop, D. (2002). Formation of hydrogen peroxide and hydroxyl radicals from A(beta) and alpha-synuclein as a possible mechanism of cell death in Alzheimer's disease and Parkinson's disease. *Free Radic. Biol. Med.* **32**, 1076–1083.
25. Turnbull, S., Tabner, B. J., El Agnaf, O. M., Moore, S., Davies, Y. & Allsop, D. (2001). alpha-Synuclein implicated in Parkinson's disease catalyses the formation of hydrogen peroxide *in vitro*. *Free Radic. Biol. Med.* **30**, 1163–1170.
26. Munishkina, L. A., Phelan, C., Uversky, V. N. & Fink, A. L. (2003). Conformational behavior and aggregation of alpha-synuclein in organic solvents: modeling the effects of membranes. *Biochemistry*, **42**, 2720–2730.
27. Hokenson, M. J., Uversky, V. N., Goers, J., Yamin, G., Munishkina, L. A. & Fink, A. L. (2004). Role of individual methionines in the fibrillation of methionine-oxidized alpha-synuclein. *Biochemistry*, **43**, 4621–4633.
28. Yamin, G., Glaser, C. B., Uversky, V. N. & Fink, A. L. (2003). Certain metals trigger fibrillation of methionine-oxidized {alpha}-synuclein. *J. Biol. Chem.* **278**, 27630–27635.
29. Wood, S. J., Wypych, J., Steavenson, S., Louis, J. C., Citron, M. & Biere, A. L. (1999). alpha-synuclein fibrillogenesis is nucleation-dependent. Implications for the pathogenesis of Parkinson's disease. *J. Biol. Chem.* **274**, 19509–19512.
30. Conway, K. A., Lee, S. J., Rochet, J. C., Ding, T. T., Williamson, R. E. & Lansbury, P. T., Jr (2000). Acceleration of oligomerization, not fibrillization, is a shared property of both alpha-synuclein mutations linked to early-onset Parkinson's disease: implications for pathogenesis and therapy. *Proc. Natl Acad. Sci. USA*, **97**, 571–576.
31. Krishnan, S., Chi, E. Y., Wood, S. J., Kendrick, B. S., Li, C., Garzon-Rodriguez, W. *et al*. (2003). Oxidative dimer formation is the critical rate-limiting step for Parkinson's disease alpha-synuclein fibrillogenesis. *Biochemistry*, **42**, 829–837.
32. Souza, J. M., Giasson, B. I., Chen, Q., Lee, V. M. & Ischiropoulos, H. (2000). Dityrosine cross-linking promotes formation of stable alpha -synuclein polymers. Implication of nitrative and oxidative stress in the pathogenesis of neurodegenerative synucleinopathies. *J. Biol. Chem.* **275**, 18344–18349.
33. Naiki, H., Higuchi, K., Hosokawa, M. & Takeda, T. (1989). Fluorometric determination of amyloid fibrils *in vitro* using the fluorescent dye, thioflavin T. *Anal. Biochem.* **177**, 244–249.
34. Naiki, H., Higuchi, K., Matsushima, K., Shimada, A., Chen, W. H., Hosokawa, M. & Takeda, T. (1990). Fluorometric examination of tissue amyloid fibrils in murine senile amyloidosis: use of the fluorescent indicator, thioflavine T. *Lab. Invest.* **62**, 768–773.
35. Nielsen, L., Khurana, R., Coats, A., Frokjaer, S., Brange, J., Vyas, S. *et al*. (2001). Effect of environmental factors on the kinetics of insulin fibril formation: elucidation of the molecular mechanism. *Biochemistry*, **40**, 6036–6046.
36. Oberg, K., Chrunyk, B. A., Wetzel, R. & Fink, A. L. (1994). Nativelike secondary structure in interleukin-1 beta inclusion bodies by attenuated total reflectance FTIR. *Biochemistry*, **33**, 2628–2634.
37. Yamin, G., Uversky, V. N. & Fink, A. L. (2003). Nitration inhibits fibrillation of human alpha-synuclein *in vitro* by formation of soluble oligomers. *FEBS Letters*, **542**, 147–152.
38. Schiller, P. W., Natarajan, S. & Bodanszky, M. (1978). Determination of the intramolecular tyrosine-tryptophan distance in a 7-peptide related to the C-terminal sequence of cholecystokinin. *Int. J. Pept. Protein Res.* **12**, 139–142.

Edited by K. Kuwajima

(Received 13 May 2005; received in revised form 17 August 2005; accepted 20 August 2005)
Available online 6 September 2005